

This article has been published in a revised form in Parasitology [http://doi.org/10.1017/S0031182015001997]. This version is free to view and download for private research and study only. Not for re-distribution, re-sale or use in derivative works. © 2017 Cambridge University Press



CAMBRIDGE
UNIVERSITY PRESS

Presence of a isoform of H⁺-pyrophosphatase located in the alveolar sacs of a scuticociliate parasite of turbot and its physiological transcendence

Journal:	<i>Parasitology</i>
Manuscript ID	PAR-2015-0303
Manuscript Type:	Research Article - Standard
Date Submitted by the Author:	17-Sep-2015
Complete List of Authors:	Mallo, Natalia; University of Santiago de Compostela, Microbiology and Parasitology Lamas, Jesús; University of Santiago de Compostela, Departament of Cellular Biology and Ecology de Felipe, Ana; University of Santiago de Compostela, Microbiology and Parasitology De Castro, María; University of A Coruña, Cellular and Molecular Biology Sueiro, Rosa; University of Santiago de Compostela, Microbiology and Parasitology Leiro, Jose; Universidad de Santiago de Compostela, Instituto Análisis Alimentarios;
Key Words:	H ⁺ -PPase, Philasterides dicentrarchi, alveolar sacs, osmoregulation, turbot

SCHOLARONE™
Manuscripts

1 Presence of an isoform of H⁺-pyrophosphatase located in the alveolar sacs
2 of a scuticociliate parasite of turbot and its physiological transcendence

3
4 NATALIA MALLO¹, JESÚS LAMAS², A. PAULA DE FELIPE¹, M. EUGENIA DE CASTRO³,
5 ROSANA SUEIRO^{1,2}, JOSÉ M. LEIRO^{1,*}

6
7 ¹*Departamento de Microbiología y Parasitología, Instituto de Investigación y Análisis Alimentarios,*
8 *Universidad de Santiago de Compostela, 15782 Santiago de Compostela, Spain*

9 ²*Departamento de Biología Celular y Ecología, Facultad de Biología, Universidad de Santiago de*
10 *Compostela, 15782 Santiago de Compostela, Spain*

11 ³*Departamento de Biología Celular y Molecular, Facultad de Ciencias, Universidad de A Coruña, 15701*
12 *A Coruña, Spain*

13
14 SHORT TITLE: **Two isoforms of inorganic pyrophosphatase in *Philasterides***
15 ***dicentrarchi***

16
17 *Correspondence to: José M. Leiro, Laboratorio de Parasitología, Instituto de Investigación y Análisis
18 Alimentarios, c/ Constantino Candeira s/n, 15782, Santiago de Compostela (A Coruña), Spain; Tel:
19 34981563100; Fax: 34881816070; E-mail: josemanuel.leiro@usc.es

20
21

22 SUMMARY

23 H^+ -pyrophosphatases (H^+ -PPases) are integral membrane proteins that couple PPi
24 energy with an electrochemical gradient across biological membranes and promoted the
25 acidification of cellular compartments. In eukaryotes organisms, essentially plants and
26 protozoan parasites, has been described the existence of various types of H^+ -PPases
27 associated to vacuoles, plasma membrane and acidic Ca^{+2} storage organelles called
28 acidocalcisomes. In this study we achieve to draw, by staining with pH sensitive dye
29 LysoTracker Red DND 99, the existence of two acidic cellular compartments in
30 trophozoites of the scuticociliate marine parasite *Philasterides dicentrarchi*: the
31 phagocytic vacuoles and the alveolar sacs. These compartments also present in its
32 membranes H^+ -PPase, which could be related with this enzyme promoting acidification
33 of these cell structures. Furthermore, we demonstrate for the first time that the *P.*
34 *dicentrarchi* H^+ -PPase is constituted by two isoforms of which one, is probably
35 generated by alternative splicing, it is localized in the membranes of the alveolar sacs
36 showing an amino acid motif recognized by the H^+ -PPase-specific antibody PAB_{HK}, and
37 it has a high degree of conservation between aa sequences of different strains of this
38 ciliate. Gene expression of H^+ -PPase is significantly regulated by variation in salinity,
39 indicating the role of this enzyme and the alveolar sacs in osmoregulation and salt
40 tolerance in *P. dicentrarchi*.

41

42 **Keywords:** H^+ -PPase, *Philasterides dicentrarchi*, alveolar sacs, osmoregulation.

43

44

45 KEY FINDINGS

- 46 • *Philasterides dicentrarchi* has at least two isoforms of H⁺-PPase
- 47 • The alveolar sacs are acidic structures containing an isoform of the H⁺-PPase
- 48 • The H⁺-PPase of the alveolar sacs is associated with a osmoregulatory function

49

50 INTRODUCTION

51 Proton-translocating inorganic pyrophosphatases (H⁺-PPases) are extremely
52 hydrophobic integral membrane proteins that utilizes the energy released upon
53 hydrolysis of pyrophosphate (PPi), that has a high-energy phosphoanhydride bond, to
54 transport H⁺ across the biological membranes against the electrochemical potential
55 gradient (Maeshima, 2000; Belogurov and Lahti, 2002; Gaxiola *et al.* 2007; Serrano *et*
56 *al.* 2004). The first discovered H⁺-PPase in membranes isolated from the
57 photosynthetic bacterium *Rhodospirillum rubrum* (Baltscheffsky *et al.* 1966), later it was
58 located in homogenates and in higher plant vacuoles (V-H⁺-PPases) as a proton pump
59 (Karlsson, 1975), and more recently was found in acidocalcisomes of parasitic protozoa
60 (Scott *et al.* 1998). Although for a long time it was considered that this enzyme was
61 present only in plants and some photosynthetic bacteria (Drozdowicz *et al.* 2003.), it has
62 now been identified in a wide range of organisms including prokaryotes extremophiles,
63 fungi, some algae and protozoa (Maeshima 2000; Drozdowicz and Rea, 2001). In
64 plants, V-H⁺-PPases are present, in addition to the vacuole membrane (tonoplast), also
65 in the plasma membrane (Rea and Poole, 1993; Long *et al.* 1995; Robinson *et al.* 1996).
66 In protozoans, V-H⁺-PPase is an integral membrane-associated protein that has been
67 localized, besides to the acidocalcisomes, within the Golgi, plasma membrane, digestive
68 vacuoles and within a microneme maturation vacuolar compartment of apicomplexans
69 (Harper *et al.* 2006).

70 The first indication of the existence of the diversity and functional heterogeneity
71 of V-H⁺-PPases was performed at the plant *Arabidopsis thaliana* observing the presence
72 of two distinct categories of the enzyme: the AVP1 and AVP2 that, after the phylogenetic
73 analyses with other V-H⁺-PPases, showing that AVP2, rather than being an isoform of
74 AVP1, is but one representative of a novel category of AVP2-like (type II) V-PPases
75 that coexist with AVP1-like (type I) V-H⁺-PPases not only in plants, but also in
76 apicomplexan protists such as the malarial parasites (Drozdowicz *et al.* 2000). Although
77 there is a clear evidence for a wide occurrence of V-H⁺-PPase genes in ciliates
78 hymenostomatids, peritrichs and hypotrichs (Pérez-Castiñeira *et al.* 2002); however,
79 until recently has only been shown the presence of V-H⁺-PPase activity in the
80 scuticociliate parasite of turbot *Philasterides dicentrarchi* (Mallo *et al.* 2015).

81 More specifically, in this work we report the results of a study that show for the
82 first time the existence of a sequence variant in genes encoding two isoforms of H⁺-
83 PPase in *P. dicentrarchi*. One of these isoforms of the enzyme are predominant located
84 in flat cortical sacs, designed “alveolar sacs” in Ciliophora, and their gene expression
85 were modulated for the salt concentration.

86

87 MATERIALS AND METHODS

88 *Parasites and experimental animals*

89 Specimens of *P. dicentrarchi* (isolates B1, C1, D2, D3, I1, S1, P1; Iglesias *et al.* 2001;
90 Budiño *et al.* 2011) were collected under aseptic conditions from ascitic fluid removed
91 from the intraperitoneal cavity of experimentally infected turbot, *Scophthalmus*
92 *maximus*, as previously described (Paramá *et al.* 2003). The ciliates were cultured at 21°C
93 in complete sterile L-15 medium as previously described (Iglesias *et al.* 2003). In order
94 to maintain the virulence of the ciliates, fish were experimentally infected every 6

95 months by intraperitoneal injection of 200 μ L of sterile physiological saline containing
96 5×10^5 trophozoites, and the ciliates were recovered from ascitic fluid and maintained in
97 culture as described above

98 Turbot, of approximately 50 g body weight, were obtained from a local fish
99 farm. The fish were kept in 250-L tanks with recirculating, aerated sea water at 14 °C,
100 subjected to a photoperiod of 12L:12D, and fed daily with commercial pellets
101 (Skretting, Burgos, Spain). Fish were acclimatized to laboratory conditions for 2 weeks
102 before the experiments were started.

103 Eight to 10- week-old ICR (Swiss) CD-1 mice initially supplied by Charles
104 River Laboratories (USA) were bred and maintained in the Central Animal Facility of
105 the University of Santiago de Compostela (Spain) following the criteria of protection,
106 control, care and welfare of animals and the legislative requirements relating to the use
107 of animals for experimentation (EU Directive 86/609 / EEC), the Declaration of
108 Helsinki, and/or the Guide for the Care and Use of Laboratory Animals as adopted and
109 promulgated by the US National Institutes of Health (NIH Publication No. 85-23,
110 revised 1996). The Institutional Animal Care and Use Committee of the University of
111 Santiago de Compostela approved all experimental protocols.

112

113 *PCR, RT-PCR, RT-qPCR*

114 *P. dicentrarchi* DNA was purified with DNAeasy Blood and Tissue Kit (Qiagen)
115 following the manufacturer's instructions. DNA was analyzed to estimate its quality,
116 purity and concentration by A_{260} measurement in a NanoDrop ND-1000
117 Spectrophotometer (NanoDrop Technologies, USA.)

118 Total RNA was isolated of *P. dicentrarchi* trophozoites with a NucleoSpin RNA
119 kit (Macherey-Nagel, Düren, Germany), following the manufacturer's instructions after

24 hours of trophozoites incubation in culture media with different saline concentrations: 4, 8 y 37 ‰. After RNA purification, quality, purity and concentration were measured with NanoDrop ND-1000 Spectrophotometer (NanoDrop Technologies, USA). For the cDNA synthesis (25 µL/reaction mixture), it was employed a reaction mix containing: 1.25 µM random hexamer primers (Promega), 250 µM each deoxynucleoside triphosphate (dNTP), 10mM dithiothreitol (DTT), 20U of RNase inhibitor, 2.5mM MgCl₂, 200U of MMLV (Moloney murine leukemia virus reverse transcriptase (Promega) in 30mM Tris and 20mM KCl (pH 8.3) and 2 µg of sample RNA. PCR (for DNA and cDNA amplification) was executed with gene-specific primers for the H⁺PPase gene: forward/reverse primer pair (FPiPh/RPiPh) 5'-CGGGACCAGAGGTATCTTTTA-3' / 5'-ATTGATGTCAACGCCCCCTT-3'; and forward/ reverse primer pair (F1qPiPh/R1qPiPh) 5'-GCCTACGAAATGGTCGAAGA-3' / 5'-GCATCGGTGTATTGTCCAGA-3' for quantitative real-time reverse transcriptase PCR (RT-qPCR). In parallel, a PCR with primers for the β-tubulin gene (forward/reverse primer pair, 5'-ACCGGGGAATCTTAAACAGG-3' / 5'-GCCACCTTATCCGTCCACTA-3') was done to use β-tubulin as a reference gene (RT-qPCR). For the design and optimization of the primer sets, Primer 3Plus program was utilized, based on default parameters. PCR mixtures (25 µL) contained PCR reaction buffer (10 mM Tris-HCl, 50 mM KCl, 1.5 mM MgCl₂, pH 9.0), 0.2 mM of each deoxynucleoside triphosphate (dNTPs, Roche), 0.4 mM of each primer, 3 units of recombinant Taq polymerase (NZY Taq DNA polymerase, Nzytech, Portugal) and 50 ng of genomic DNA or 2µL of cDNA. The reactions were run in automatic thermocycler (Biometra, Germany) as follows: initial desnaturing at 94°C for 5 min; then 35 cycles at 94°C for 30 s, 57°C for 45 s, and 72°C for 1 min; and finally a 7 min extension phase at 72°C. qPCR mixtures (10 µL) contained 5-µL Maxima SYBR green

qPCR Master Mix (Thermo Scientific), the primer pair at 300 nM, 1 µL of cDNA, and RNase-DNase-free water. qPCR was developed at 95°C for 5 min, followed by 40 cycles at 95°C for 10 s and 60°C for 30 s ending with a melting-curve analysis at 95°C for 15 s, 55°C for 15 s, and 95°C for 15 s. The specificity and size of PCR products were confirmed by 4% agarose gel electrophoresis. All qPCRs were performed in an Eco Real-Time PCR system (Illumina). Relative quantification of gene expression was determined by the $2^{-\Delta\Delta C_t}$ method (Livak K.J., *et al.* 2001) by using software conforming to MIQE (minimum information for publication of quantitative real-time PCR experiments) guidelines (Bustin *et al.* 2009)

154

155 *Production of recombinant H⁺-PPase of P. dicentrarchi in yeast cells*

P. dicentrarchi RNA was purified with a NucleoSpin RNA kit (Macherey-Nagel, Düren, Germany), following the manufacturer's instructions and cDNA synthesis was performed as indicated in the previous section. The PCR was carried out with gene-specific primers designed from a partial sequence of the H⁺-PPase of *P. dicentrarchi* (Mallo *et al.* 2015) (forward/reverse primer pair 5'-AAAGAAGAAGGGGTACCTTTGGATAAAAGAattgatgtcaacgccccctt-3' / 5'-TGGGACGCTCGACGGATCAGCGGCCGCTTAGTGGTGGTGGTGGTGGTggggacagaggtatctttta-3'). These primers were designed and optimized by means of the *Saccharomyces* Genome Database (<http://www.yeastgenome.org/>) including a hybridization region with the yeast YEpFLAG-1 (Eastman Kodak Company) plasmid and a poly His region (lower case letters correspond with the gene annealing zone). PCR reaction was developed initially at 95 °C for 5 min, and then for 30 cycles of 94 °C for 1 min, 55 °C for 1.5 min and 72 °C for 2 min. After the 30 cycles, a 7-min extension phase at 72 °C was carried out. The PCR products were purified using Gene Jet PCR

170 Purification Kit (Fermentas, Life Sciences) according with the manufacturer's
171 instructions.

172 Purified PCR products were cloned in YEpFLAG-1 (Eastman Kodak Company)
173 yeast expression vector, a plasmid that carries a TRP1 gene that completes the
174 auxotrophy for the tryptophan for the host yeast (López-López *et al.* 2010).

175 Linearized plasmid YEpFLAG-1 by digestion with *EcoRI* and *Sall* (Takara) was
176 used to transform *Saccharomyces cerevisiae* cells (strain BJ 3505) by the lithium
177 acetate procedure (Ito *et al.* 1983). The procedure involves co-transformation of yeast
178 cells with the linearized empty plasmid and the PCR-generated DNA fragment so that a
179 recombination process occurs within the cell yielding a plasmid bearing the desired
180 insert. Positive colonies were selected using complete medium without tryptophan (CM-
181 Trp) containing glucose (20g/L), Yeast Nitrogen Base without amino acids medium
182 (Sigma-Aldrich) adenine (40mg/L) and amino acids (histidine, leucine, tyrosine,
183 40mg/L each; arginine, methionine, threonine 10mg/L each; isoleucine and
184 phenylalanine 60mg/L each and lysine 40mg/L).

185 Plasmid DNA was then extracted with Easy Yeast Plasmid Isolation Kit
186 (Clontech) following the manufacturer's instructions. The purified and cloned DNA
187 fragment was subjected to sequencing analysis (Sistemas Genómicos, Spain).

188 Recombinant protein of H⁺-PPase of *P. dicentrarchi* was purified from
189 transformed *Saccharomyces cerevisiae* cultures, after 72h in modified Yeast Peptone
190 High Stability Expression Medium (YPHSM) containing 1% glucose, 3% glycerol, 1%
191 yeast extract, and 8% peptone, at 30°C in Erlenmeyer flasks filled with 20% volume of
192 culture medium at 250 rpm (López-López *et al.* 2010). As inoculum, a suitable volume
193 of a pre-culture was added to obtain an initial OD₆₀₀ of 0.1. The cell suspension was
194 centrifuged at 7500g for 15 min and the cleared supernatant was purified by

195 immobilized metal affinity chromatography on a pre-charged Ni-Sepharose Histrap
196 column (ÄKTAprime plus, GE Healthcare Life Sciences). The column was initially
197 equilibrated with 25 mL of binding buffer (20 mM sodium phosphate, 0.5 M NaCl, 20
198 mM imidazole, pH 7.4). After the equilibration 100mL of culture medium were charged
199 through the column and finally, the protein bound to the column was eluted in 10 mL of
200 elution buffer (20mM sodium phosphate, 0.5 M NaCl, 250 mM imidazole, pH 7.4)
201 ([Mallo *et al.* 2015](#)) Fractions from the elution were analyzed by 12.5% SDS-PAGE and
202 dialyzed overnight in 2 L of bidistilled water. The dialyzed sample was concentrated in
203 an Amicon Ultra centrifugal filter device (Millipore, USA) with a 10-kDa cut-off
204 membrane. The final protein concentration was calculated by the Bio-Rad Protein
205 Assay, which is based on the Bradford assay (Bradford, 1976).

206

207 *Peptide synthesis*

208 A peptide of 17 amino acids long corresponding to domain HKAAVIGDTIGDPLKDT
209 (PAB_{HK}) of the *P. dicentrarchi* H⁺-PPase were synthesized and conjugated to keyhole-
210 limpet hemocyanin (KLH), a carrier protein, to assure maximum immunogenicity
211 (ProteoGenix, France). A cysteine amino acid was added to two sequences to allow
212 conjugation to KLH. The peptide were synthesized and conjugated to KLH by coupling
213 agent sulfo-SMCC at a yield of 10-20 mg having >85% purity, lyophilized and stored at
214 -20°C until use.

215

216 *Immunization and serum extraction*

217 A group of five ICR (Swiss) CD-1 mice were immunized by i.p. injection with 200µL
218 per mouse of a 1:1 (v/v) mixture of Freund complete adjuvant (Sigma-Aldrich) and a
219 solution containing 500 µg of purified recombinant H⁺-PPase and 400 µg of synthetic

220 peptide in PBS. The same dose of purified protein and peptide was prepared in Freund's
221 incomplete adjuvant and injected i.p in mice 15 and 30 days after the first
222 immunization. The mice were bled via retrobulbar venous plexus 7 days after the
223 secondary immunization (Piazzon *et al.* 2011). The blood was left to coagulate
224 overnight at 4° C before the serum was separated by centrifugation (2000 × g for 10
225 min), mixed 1:1 with glycerol and stored at −20°C until use. In some experiments, a
226 commercial rabbit polyclonal serum against KLH-conjugated synthetic peptide derived
227 from *Arabidopsis thaliana* V-PPase, (anti-AVP1; UniProt P311414; Agrisera, Sweden)
228 was also used.

229

230 *Western-blot analysis*

231 Ciliate membrane-associated proteins (MAPs) were extracted by phase separation in
232 Triton X-114 solution (Bordier, 1981), by a previously described method (Mallo *et al.*
233 2013). Specifically, 10⁷ cells were resuspended in 1 ml of ice-cold 10 mM Tris–HCl
234 buffer, pH 7.5, to which 1 ml of ice-cold extraction buffer (300 mM NaCl, 20 mM Tris–
235 HCl, pH 7.5, 2% Triton X-114) was subsequently added. The cytoskeletal elements
236 were eliminated by centrifugation at 16000 x g for 10 min at 4 °C. The supernatant was
237 then transferred to 1.5 ml Eppendorf tubes, which were heated for 5 min at 37 °C. At the
238 end of this period, the solution became cloudy as a result of condensation of detergent
239 micelles. The sample was then placed in 0.5 ml Eppendorf tubes (200 μ l/tube)
240 containing 300 μ l of sucrose cushion (6% sucrose, 150 mMNaCl, 10 mMTris–HCl, pH
241 7.5, 0.06% Triton X-114). The detergent and aqueous phases were separated by
242 centrifugation at 300 g for 4 min at room temperature. The resulting supernatants on the
243 sucrose cushion of each tube were extracted carefully and mixed in new 1.5 ml
244 Eppendorf tubes. The extraction process was repeated by adding sufficient Triton X-114

245 to the aqueous mixture to obtain a final concentration of 0.5%. The mixture was re-
246 heated at 37 °C for 5 min. Once micellar condensation had taken place, the mixture was
247 distributed among the original Eppendorf tubes containing the sucrose cushion and the
248 detergent phase separated in the first extraction. The tubes were then recentrifuged at
249 300 g for 4 min at room temperature. The resulting supernatant was discarded and the
250 proteins contained in the detergent phase were precipitated, by adding 9 volumes of cold
251 acetone, resuspended, by vortexing, and finally incubated for 30 min on ice. The
252 precipitated membrane proteins were then collected by centrifugation at 16000 g for 15
253 min at 4 °C and dried in a speed vacuum concentrator (MiVac, GeneVac, UK). Finally,
254 the extracts obtained were resuspended in 10 mM Tris-HCl, pH 7.5, and stored at -80
255 °C until use. The protein concentration of preparation was determined by Bradford
256 assay.

257 Samples from MAPs were separated under non-reducing conditions by linear
258 SDS-PAGE 12.5 % gels (Piazzon *et al.* 2008). After the electrophoresis, the gels were
259 stained with Thermo Scientific GelCode Blue Safe Protein Stain (Thermo Fisher, USA)
260 to determine qualitatively the protein bands. In parallel, a gel was submitted to
261 immunoblotting at 15 V for 35 min to Immobilon-P transfer membranes (0.45 μ m;
262 Millipore, USA) in a trans-blot SD transfer cell (Bio-Rad, USA) with the transference
263 buffer (48 mM Tris, 29 mM glycine, 0.037% SDS and 20% methanol, pH 9.2). The
264 membrane was washed with Tris buffer saline (TBS; 50 mM Tris, 0.15 M NaCl, pH
265 7.4) and immediately stained with Ponceau S to verify transfer. After membrane
266 destaining with bidistilled water, a blocking solution containing 0.2% Tween 20 and 3%
267 BSA with TBS was added and the membrane was incubated for 1.5 h at room
268 temperature. Then, it was washed in TBS and incubated overnight with anti-PAB_{HK} at
269 1:100 dilutions, at 4°C. Subsequently; the membrane was washed with TBS and

270 incubated with rabbit anti-mouse IgG (Dakopatts; dilution 1:6000) for 1 h at room
271 temperature. Once the membrane was washed 5 times for 5 min with TBS, it was
272 incubated for 1 min with enhanced luminol-based chemiluminiscent substrate (Pierce
273 ECL Western Blotting Substrate, Thermo Scientific, USA) and then visualized and
274 photographed with a FlourChem® FC2 imaging system (Alpha Innotech, USA).

275

276 *Immunofluorescence, Immunoelectron microscope and fluorescent stain with pH-*
277 *sensitive dye*

278 For immunolocalization of H⁺-PPase isoforms, an immunofluorescence assay was
279 performed following the protocol described previously (Mallo *et al.* 2015). Briefly,
280 5x10⁶ ciliates were centrifuged at 750 x g for 5 min, washed twice with Dulbecco's
281 phosphate buffered saline (DPBS, Sigma Aldrich) and fixed for 5 min in a solution of
282 4% formaldehyde in DPBS. Following fixation, ciliates were washed twice with DPBS,
283 resuspended in a solution containing 0.1% Triton X-100 (PBT) for 3 min and then
284 washed twice with DPBS. Ciliates were then incubated with 1% bovine serum albumin
285 (BSA) for 30 min. After blocking, ciliates were incubated at 4°C overnight with a
286 solution containing 1:100 dilutions of anti-H⁺-PPase form recombinant yeast antibody
287 and anti-PAB_{HK}. Then, ciliates were washed 3 times with DPBS followed by 1 h
288 incubation, at room temperature; with a 1:100 dilution of FITC conjugated rabbit/goat
289 anti-mouse/rabbit IgG-FITC antibody (Sigma). After three in DPBS, the samples were
290 double stained with 0.8 mg/mL 4', 6-diamidine-2-phenylindole (DAPI; Sigma-Aldrich)
291 in DPBS for 15 min at room temperature (Paramá *et al.* 2007). After three washes with
292 DPBS samples were mounted in PBS-glycerol (1:1) and visualized by fluorescence
293 microscopy (Zeiss Axioplan, Germany) and/or confocal microscopy (Leica TCS-SP2,
294 LEICA Microsystems Heidelberg GmbH, Mannheim, Germany).

295 For immunoelectron microscopy, 5×10^6 ciliates from cultures in exponential
296 growth phase were centrifuged at $750 \times g$ for 5 min and washed in two changes of
297 Sørensen buffer (SB; 0.1 M sodium/potassium phosphate buffer, pH 7.3) at room
298 temperature (RT). The resulting pellet were fixed for 60 min in 4% paraformaldehyde
299 and 0.1% glutaraldehyde in SB at 4°C. After the fixation, samples was washed in two
300 changes of SB (10 min each) and incubated with 0.02 M glycine in SB for 10 min at
301 RT. Ciliates were dehydrated in series of pre-cooled ethanol solutions (30, 50, 70, 80,
302 96 and 100% of 10 min each). After dehydration, the pellet were included in a mix of
303 ethanol and resin (LR White uncatalized, Santa Cruz Biotechnology, USA;
304 [Philimonenko et al. 2002](#)) 2:1 for 20 min and pure resin for 2 h. Samples were infiltrate
305 overnight with fresh resin at 4°C. The next day, a new exchange of fresh resin was made
306 and allowed to polymerize at 65 °C in vacuum for 48h. Thin sections (80 nm thick)
307 were cut with a diamond knife on a Reichert Ultracut E (Leica Microsystems AG,
308 Germany). Thin sections were collected on 300 mesh nickel grids (Sigma-Aldrich) and
309 was blocked by preincubation with 10% normal goat serum (NGS) in PBS-10%
310 albumin and 0.1% Tween-20 (PBTB) for 30 min at RT. The sections were incubated for
311 1 h with a primary polyclonal antibody anti-AVP1 diluted in PBTB at 1:100 dilution,
312 washed in PBS-albumin, and incubated with 10 nm gold-labeled goat anti-rabbit IgG
313 (Sigma) at 1:50 dilution for 60 min. Finally the sections were washed in distilled water,
314 stained with uranyl acetate and lead citrate, and observed with a JEOL-JEM-2010
315 transmission electron microscope operating at 120 kV (JEOL, Japan). Controls were
316 carried out using a non-related antibody or incubation in the presence of the secondary
317 antibody only.

318 For identification of the acidic compartments on trophozoites of *P. dicentrarchi*
319 we used a fluorescent stain assay with pH-sensitive dye LysoTracker Red DND-99.

320 5×10^5 ciliates were centrifuged at $700 \times g$ for 5 min and washed twice with PBS
321 followed by a 10 min staining with 75 nM LysoTracker Red DND-99 (Lifetechnologies)
322 solution. After staining, ciliates were observed in a fluorescence microscopy with an
323 excitation filter BP 546 nm, dichroic mirror FT 580 nm and emission filter LP 590 nm.

324

325 *Bioinformatic and statistical analysis*

326 The aminoacid sequences obtained for the H^+ -PPase gene were aligned with the
327 multiple alignments Clustal Omega program (Sievens *et al.* 2011). Genetic distances
328 were calculated to quantify sequences divergences among isolates by use of Kimura's
329 (1980) two-parameter model, as implemented in MEGA versión 6.0 (Tamura *et al.*
330 2013). Phylogenetic tree were constructed with the MEGA programme, by the
331 neighbour-joining (NJ) method applied to the Kimura two-parameter correction model
332 (Kimura 1980) by bootstrapping with 1000 replicates (Felsenstein, 1985).

333 The results are expressed as means \pm standard error of the mean (S.E.M.). The
334 data were examined by one-way analysis of variance (ANOVA) followed by Tukey–
335 Kramer test for multiple comparisons, and differences were considered significant at
336 $\alpha = 0.05$.

337

338 RESULTS

339 *Cellular localization of H^+ -PPase of P. dicentrarchi in acidic compartments*

340 Initially we cloned a cDNA fragment encoding 169 aa located between positions 305
341 and 474 of the aminoacid sequence of the H^+ -PPase (GenBank accession AHH28243)
342 containing domain HKAVIGDTIGDPLKDTS in yeast expression vector YepFlag-1.
343 The mouse anti- H^+ -PPase polyclonal antibodies generated following immunization with
344 the recombinant protein fragment, produces intense fluorescent staining of vacuoles

345 located on the back half part of trophozoites and alveolar sacs located under the plasma
346 membrane (Fig. 1A).

347 Incubation of trophozoites of *P. dicentrarchi* with pH sensitive dye LysoTracker
348 Red DND-99, produces an intense staining in the vacuoles and in the alveolar sacs (Fig.
349 1B).

350

351 *Immunohistochemical pattern of the H^+ -PPase when polyclonal antibodies PAB_{HK}*
352 *were used*

353 Indirect immunofluorescence studies using a mouse polyclonal antibody generated
354 against a KLH-conjugated synthetic peptide of the conserved amino acid domain
355 HKAAVIDTIGDPLKDT (PAB_{HK}; Fig. 2A) and the polyclonal antibody anti-AVP, a
356 KLH-conjugated synthetic peptide derived from *Arabidopsis thaliana* V-PPase (Fig.
357 3B), reveal a unique labeling on the surface of the parasite appreciate clear punctate
358 staining pattern in the trophozoites of *P. dicentrarchi*. In immunoelectron microscopy
359 using the polyclonal antibody anti-AVP1 clearly shows specific labeling in the
360 membranes of the alveolar sacs (Fig. 3 C-D).

361

362 *Sequence characteristics of H^+ -PPase isoforms*

363 To investigate the possible existence of various types of H^+ -PPase in *P. dicentrarchi*
364 located in the posterior vacuoles and in the alveolar sacs, we amplified a fragment of
365 this gene by PCR and have also generated several cDNA from RNA using the pair of
366 primers FPiPh/RPiPh. In Figure 3A, the results of nucleotide sequence amplified by
367 PCR corresponding to an partial open reading frame (ORF) of H^+ -PPase gene and its
368 amino acid translation are shown. When analyzing on agarose gel 4% the DNA
369 fragment amplified with primers FPiPh / RPiPh, the appearance of a single band of 558

nucleotides in size was observed; however, when a cDNA is generated from total RNA by RT-PCR and amplified with the same primers, two bands were obtained, one with an identical size to that obtained after DNA amplification (558 nucleotides) and a second band of 495 nucleotides (Fig. 3A). The sequencing of the two bands obtained by RT-PCR showed that the nucleotide sequence of the larger fragment corresponded exactly to the sequence obtained by PCR from genomic DNA, whereas the sequencing of the minor band showed the disappearance of 63 nucleotides which is located in the largest band. After translation to aa of the two amplified fragments by RT-PCR, shows that the lower band produces a protein containing the domain complete HKAAVIGDTIGDPLKDTS, while the largest band generates a protein with this fragmented domain, containing an internal sequence of 21 amino acids (Fig. 3A).

Polyclonal antibodies generated in mice after immunization with the synthetic peptide corresponding to domain PAB_{HK}, recognized on MAPs in Western blot a single protein band of approximately 60 kD (Fig. 3B).

Phylogenetic analysis of H⁺-PPases in several strains of P. dicentrarchi

To determine the degree of phylogenetic evolution between isolates of *P. dicentrarchi*, we amplified by PCR the DNA of seven isolates using the primers pair FPiPh / RPiPh. After obtaining the nucleotide sequence of each isolate and its translation into aa, was carried out a multiple alignment of the amino acid sequences using the Clustal Omega program, showing a very high degree of conservation between aa sequences of the isolates analyzed (Fig. 4A). This high level of conservation in aa sequences results in the existence of a low genetic distance between isolates and, when the phylogenetic tree using the NJ method is constructed, it is noted that five isolates have 100% homology (I1, B1, D3, P1 and S1 isolates), whereas D2 and C1 constitute two phylogenetically different groups (Fig. 4B).

396

397 *Effect of salt concentration on the expression of H^+ -PPase*

398 The assays on the expression levels of RNA corresponding to the H^+ -PPase of *P.*
399 *dicentrarchi* trophozoites cultivated in a saline medium containing different
400 concentrations of NaCl: between 4, 8 and 37 ‰, are shown in Fig.5. Relative mRNA
401 levels, quantified by qPCR, of H^+ -PPase remain unchanged at NaCl concentrations
402 between 8 and 37 ‰; however when the medium contains low concentrations of NaCl
403 (such as 4‰), a significant increase in the expression of H^+ -PPase, relative to levels
404 obtained in ciliates then incubated at concentrations of NaCl between 8 and 37 ‰ (Fig.
405 5).

406

407 DISCUSSION

408 H^+ -PPases are enzymes that translocates H^+ across a membrane by using potential
409 energy liberated on hydrolysis of the phosphoanhydride bond of inorganic phosphate
410 (Read and Poole, 1993). They are widely distributed among land plants and have been
411 found in several of protozoan parasites including the scuticociliate parasite of turbot, *P.*
412 *dicentrarchi* (Mallo *et al.* 2015). In eukaryotes, H^+ -PPases are associated to certain
413 acidic compartments of the endomembrane system, namely, the vacuole and lysosomes
414 of plant cells and the acidocalcisomes of trypanosomatids and apicomplexans
415 protozoan (Pérez-Castiñeira *et al.* 2002; Scott and Docampo, 2000; Docampo *et al.*
416 2005). Some functions of the acidocalcisomes are the storage of cations, Ca^{2+}
417 homeostasis, maintenance of intracellular pH homeostasis and osmoregulation (Moreno
418 and Docampo, 2009). In parasitic protozoans, acidocalcisomes also interact with other
419 organelles as the contractile vacuole and other vacuoles associated with the
420 endosomal/lysosomal pathway (Moreno and Docampo, 2009; Docampo *et al.* 2010). In

ciliates, such as *Paramecium caudatum*, has been described acidification of phagocytic vacuoles occurs through fusion nonlysosomal vesicles, named acidosomes, with the newly released vacuoles and these vesicles accumulate neutral red as well as acridine orange, two observations that demonstrate their acid content (Allen and Fok, 1983). Sequencing of the whole genome of several species of ciliates enable the identification of genes encoding the V-ATPase, a proton pump that drives H^+ across membranes, and that is crucial as an acidifier of food vacuoles (Plattner, 2010); however, although there is evidence of the existence of H^+ -PPases in ciliates, since there are several sequences deposited in nucleotide databases (eg. *Tetrahymena thermophila*, GenBank accession XM_001011583; *Tetrahymena pyriformis*, GenBank accession AJ251772), it available thus far too little information on the occurrence of membrane-bound H^+ -PPases and their physiological role in these Protozoa (Pérez-Castiñeira *et al.* 2001). Although acidocalcisomes as a whole and some of their transport activities have not been characterized in ciliates as yet, where they may also occur (Plattner *et al.* 2012). In this study it is clearly evident that the H^+ -PPase in *P. dicentrarchi* colocalises both phagocytic vacuoles and in the alveolar sacs, and these two structures are acidic cellular components which are stained with the pH sensitive dye LysoTracker Red DND 99.

Although subcellular localization of members of the H^+ -PPase family is mainly in endocellular membranes (vacuolar tonoplast) and acidocalcisomal membranes of eukaryotes (algae, plants and protozoa) (Maeshima, 2000; Drozdowicz and Rea, 2001; Docampo *et al.* 2005) and plasma membrane invaginations of both bacteria and archaea (Baltscheffsky *et al.* 1999; Serrano *et al.* 2004), evidence for a differential subcellular localization of the AVP1 (vacuole) and AVP2 (Golgi complex and lysosomes) isoforms has been only reported in plant cells (Rea *et al.* 1992; Mitsuda *et al.* 2001). Indirect immunofluorescence microscope with polyclonal antibodies to investigate the

subcellular localization of V-H⁺-PPase in *P. falciparum* indicated that VP1 is present within the vacuolar membrane and, possibly, in food vacuoles (Luo *et al.* 1999; MacIntosh *et al.* 2001) and it seems that the proton pumps V-H⁺-PPase and V-H⁺-ATPase are colocalized in acidic organelles in malarian parasites including acidocalciomes and food vacuoles (Marchesini *et al.* 2000; Saliba *et al.* 2003; Moriyama *et al.* 2003). In our study, we demonstrate by immunofluorescence and immunohistochemistry to TEM that the PAB_{HK} sera, which recognizes the highly conserved domain HKAAVIDTIGDPKDT, It generates a specific labeling only on the alveolar sacs of ciliates, which suggests that this domain is not found, or not recognized in the H⁺-PPase vacuoles. Thus, immunostaining with PAB_{HK} could be evidencing the possible existence of two isoforms of H⁺-PPase in *P. dicentrarchi*.

The existence of multiple H⁺-PPases isoforms is clearly demonstrated in plants (Venter *et al.* 2006). Thus for example, in rice (*Oryza sativa* L.) genome have been detected at least two genes encoding the H⁺-PPase (Sakakibara *et al.* 1995), three isoforms in tobacco (Lerchl *et al.* 1995), two isoforms in red beet (*Beta vulgaris* L.) (Kim *et al.* 1994), two isoforms in barley (*Hordeum vulgare* L.) (Fukuda *et al.* 2004), two isoforms in grapevine (*Vitis vinifera* L.) (Venter *et al.* 2006), two isoforms in cacao (*Theobroma cacao* L.) (Motamayor *et al.* 2013), with highly homologous within the coding region but differs strongly in the untranslated regions and their expression are probably regulated in a different manner (Maeshima, 2000). Plants have two phylogenetically distinct V-H⁺-PPases that can be classified into two subclasses, AVP1, that depend on cytosolic K⁺ for their activity and are moderately sensitive to inhibition by Ca²⁺ and AVP2, which are K⁺-independent but extremely Ca²⁺-sensitive (Sarafian *et al.* 1992; Drozdowicz *et al.* 2000; Gaxiola *et al.* 2007). Parasites, such as in the malarian parasite *Plasmodium falciparum*, also two genes encoding corresponding VP1

471 and VP2 have been identified (MacIntosh *et al.* 2001), and in ciliates also available in
472 the databases of the sequence corresponding to an isoform 2 of himenostomatid
473 *Tetrahymena pyriformis* (GenBank accession AJ251471).

474 There is a near-complete conservation between AVP1/AVP2 of the aminoacids
475 sequences recognized by polyclonal antibody PAB_{HK} (HKAAVIGDTIGPLK) that
476 provides further justification for the proposal that these antibodies are universal reagents
477 for the detection of V-PPase polypeptides (Drozdowicz and Rea, 2001). We have
478 previously shown that H⁺-PPase of *P. dicentrarchi* showed a common motif with the
479 polyclonal antibody PAB_{HK} specific to AVP1 (Mallo *et al.* 2015). Specifically, in this
480 study we found that this motif is encoded by a gene containing an intercalated
481 nucleotide sequence to be transcribed into RNA generates two isoforms: one of which
482 produces a protein with the fragmented motif and other isoform produces a protein
483 containing the complete motif. The total sizes of the proteins produced by gene
484 isoforms would vary between 62-64 kD (2kD difference is the estimated size of the
485 peptide intercalated between the motif PAB_{HK}), but an analysis by SDS-PAGE or
486 Western blot probably would go unnoticed due to the limitation of this technique for
487 separating proteins of molecular sizes very close (Daully *et al.* 2006). The hypothesis
488 proposed in this paper to explain the presence of the two H⁺-PPase isoforms is based, on
489 the one hand in the differential recognition of the H⁺-PPase in the alveolar sacs by
490 PAB_{HK} antibodies, and secondly, in the presence of two amino acid sequences in the
491 cDNAs generated by RT-PCR with primers FPiPh / RPiPh. The presence of the two
492 isoform containing the complete PAB_{HK} motif in the H⁺-PPase in the alveolar sacs
493 could be explained by the existence of an alternative splicing, while isoform 1 of H⁺-
494 PPase present in the vacuoles not suffer this process and generate a protein with
495 fragmented motif it would not be recognized by the polyclonal anti-

496 HKAAVIGDTIGPLKDT (PAB_{HK}). There are some examples of genes that generate
 497 isoforms transcribed from alternate promoter sites within the gen which may mediate
 498 cell signaling and induce their translocation to various cellular localizations (Saito *et al.*
 499 2002). Furthermore, it is also well known that the splicing regulation can be modulated
 500 by several sequence elements in both exons and introns that either activate (exonic
 501 splicing enhancer, ESE; intronic splicing enhancer, ISE), or repress (exonic splicing
 502 silencer, ESS; intronic splicing silencer, ISS) (Poulos *et al.* 2011).

503 The description of nucleotide sequences of H⁺-PPase genes from plants, bacteria
 504 and archaea brought forward an unusually high degree of sequence conservation
 505 (Serrano *et al.* 2007). In our study, we also found a high level of sequence conservation
 506 of the H⁺-PPase gene among several isolates of *P. dicentrarchi* which also could also be
 507 used, conjunction with other highly conserved genes such as the α -tubulin, for
 508 detecting intraspecific genetic variation within populations of scuticociliates that infect
 509 cultured turbot (Budiño *et al.* 2011).

510 In plants, it is well established that the efficient exclusion of Na⁺ excess from
 511 the cytoplasm and vacuolar Na⁺ accumulation are the most important steps towards the
 512 maintenance of ion homeostasis inside the cell, and both tonoplast and plasma
 513 membrane Na⁺/H⁺ antiporters exclude Na⁺ from the cytosol driven by the H⁺-motive
 514 force generated by the plasma membrane H⁺-ATPase and H⁺-PPase (Silva and Gerós,
 515 2009). Algal and plant H⁺-PPases are induced under anoxia, chilling and salt stresses
 516 (Carystinos *et al.* 1995; Fukuda *et al.* 2004), and overexpression of the vacuolar H⁺-
 517 PPase isoform AVP1 in the model plant *Arabidopsis* has been claimed to confer
 518 increased saline and drought tolerance (Gaxiola *et al.* 2001). Ciliates are eurihalins
 519 organisms particularly well adapt to salinity changes, can live in salinities as low as
 520 4‰ and as high as 62‰ (27‰ higher than seawater) (Hu, 2014). In our study, we found

that *P. dicentrarchi* is able to respond to salinity stress with changes in the expression of H^+ -PPase located in the alveolar sacs indicating a potential role of these structures in salt tolerance by marine scuticociliates.

In conclusión, the H^+ -PPase of *P. dicentrarchi* is located in the membranes of the phagocytic vacuole and alveolar sacs promoting the acidification of these cellular compartments. Specifically, in the alveolar sacs are located a isoform of ionic pump H^+ -PPase containing a highly conserved aa motif generated by alternative splicing process, that is recognized by polyclonal antibodies PAB_{HK}, and whose gene expression is regulated under conditions altered salt, which suggest that these structures must play an important physiological role in the adaptative responses of these marine ciliates to maintenance of both intracellular pH homeostasis and osmoregulation.

ACKNOWLEDGEMENTS

This study was financed by a project from the Ministerio de Economía y Competitividad (Spain) under grant agreement No. AGL 2014-57125-R, by a project from the European Union Horizon 2020 research and innovation programme under grant agreement No. 634429, and by a project from the Xunta de Galicia (Spain) under grant agreement No. GPC 2014/069.

541 REFERENCES

- 542 **Allen, R.D. and Fok, A.K.** (1983). Nonlysosomal vesicles (acidosomes) are involved
543 in phagosome acidification in *Paramecium*. *The Journal of Cell Biology* **97**, 566-
544 570.
- 545 **Baltscheffsky, H., von Stedingk, L.-V., Heldt, H.W. and Klingenberg, M.** (1966).
546 Inorganic pyrophosphate formation in bacterial photophosphorylation. *Science*
547 **153**, 1120-1122.
- 548 **Baltscheffsky, M., Schultz, A. and Baltscheffsky, H.** (1999). H⁺-PPases a tightly
549 membrane-bound family. *FEBS Letters* **457**, 527-533.
- 550 **Belogurov, G.A. and Lahti, R.** (2002). A lysine substitute for K⁺. *Journal of Biological*
551 *Chemistry* **277**, 49651-49654.
- 552 **Bordier, C.** (1981). Phase separation of integral membrane proteins in Triton X-
553 114 solution. *Journal of Biological Chemistry* **256**, 1604-1607.
- 554 **Budiño, B., Lamas, J., Pata, M.P., Arranz, J.A., Sanmartín, M.L. and Leiro, J.**
555 (2011). Intraspecific variability in several isolates of *Philasterides dicentrarchi*
556 (syn. *Miamiensis avidus*), a scuticociliate parasite of farmed turbot. *Veterinary*
557 *Parasitology* **175**, 260-272.
- 558 **Bustin, S.A., Benes, V., Garson, J.A., Hellemans, J., Huggett, J., Kubista, M.,**
559 **Mueller, R., Nolan, T., Pfaffl, M.W., Shipley, G.L., Vandesompele, J. and**
560 **Wittwer, C.T.** (2009). The MIQE guidelines: minimum information for
561 publication of quantitative real-time PCR experiments. *Clinical Chemistry* **55**,
562 611-622.
- 563 **Carystinos, G.D., McDonald, H.R., Monroy, A.F., Dhindsa, R.S. and Poole, R.J.**
564 (1995). Vacuolar H⁺-translocating pyrophosphatase is induced by anoxia or
565 chilling in seedlings of rice. *Plant Physiology* **108**, 641-649.

- 566 **Dauly, C., Perlman, D.H., Costello, C.E. and McComb, M.E.** (2006). Protein
567 separation and characterization by np-RP-HPLC followed by intact MALDI-
568 TOF mass spectrometry and peptide mass mapping analyses. *Journal of*
569 *Proteome Research* **5**, 1688-1700.
- 570 **Docampo, R., de Souza, W., Miranda, K., Rohloff, P. and Moreno, S.N.** (2005).
571 Acidocalcisomes - conserved from bacteria to man. *Nature Reviews*
572 *Microbiology* **3**, 251-261.
- 573 **Docampo, R., Ulrich, P., Moreno, S.N.J.** (2010). Evolution of acidocalcisomes and
574 their role in polyphosphate storage and osmoregulation in eukaryotic microbes.
575 *Philosophical Transactions of Royal Society B* **365**, 775-784.
- 576 **Drozdowicz, Y.M., Kissinger, J.C. and Rea, P.A.** (2000). AVP2, a sequence-
577 divergent, K^+ insensitive H^+ -translocating inorganic pyrophosphatase from
578 *Arabidopsis*. *Plant Physiology* **123**, 353-362.
- 579 **Drozdowicz, Y.M. and Rea, P.A.** (2001). Vacuolar H^+ pyrophosphatases: from the
580 evolutionary backwaters into the mainstream. *Trends in Plant Science* **6**, 206-
581 211.
- 582 **Drozdowicz, Y.M., Shaw, M., Nishi, M., Striepen, B., Liwinski, H.A., Roos, D.S.**
583 **and Rea, P.A.** (2003). Isolation and characterization of TgVP1,
584 a type I vacuolar H^+ -translocating pyrophosphatase from *Toxoplasma gondii*.
585 The dynamics of its subcellular localization and the cellular effects of a
586 diphosphonate inhibitor. *The Journal of Biological Chemistry* **278**, 1075-1085.
- 587 **Felsenstein, J.** (1985). Confidence limits on phylogenies: and approach using the
588 bootstrap. *Evolution* **39**, 783-791.
- 589 **Fukuda, A., Chiba, K., Maeda, M., Nakamura, A., Maeshima, M., Tanaka, Y.**
590 (2004). Effect of salt and osmotic stresses on the expression of gene for the

- 591 vacuolar H⁺-pyrophosphatase, H⁺-ATPase subunit A, and Na⁺/H⁺ antiporter from
 592 barley. *Journal of Experimental Botany* **55**, 585-594.
- 593 **Gaxiola, R.A., Li, J., Undurraga, S., Dang, L.M., Allen, G., Alper, S.L. and Fink,**
 594 **G.R.** (2001). Drought- and salt-tolerant plants result from overexpression of the
 595 AVP1 H⁺-pump. *Proceedings of the National Academy of Sciences USA* **98**,
 596 11444-11449.
- 597 **Gaxiola, R.A., Palmgren, M.G. and Schumacher, K.** (2007). Plant proton pumps.
 598 *FEBS Letters* **581**, 2204-2214.
- 599 **Harper, J.M., Huynh, M.H., Coppens, I., Parussini, F., Moreno, S., Carruthers,**
 600 **V.B.** (2006). A cleavable propeptide influences *Toxoplasma* infection by
 601 facilitating the trafficking and secretion of the TgMIC2-M2AP invasion
 602 complex. *Molecular Biology of the Cell* **17**, 4551–4563.
- 603 **Hu, X.** (2014). Ciliates in extreme environments. *Journal of Eukaryotic Microbiology* **61**,
 604 410-418.
- 605 **Iglesias, R., Paramá, A., Álvarez, M.F., Leiro, J., Fernández, J. and Sanmartín,**
 606 **M.L.** (2001) *Philasterides dicentrarchi* (Ciliophora, Scuticociliatida) as the
 607 causative agent of scuticociliatosis in farmed turbot *Scophthalmus maximus* in
 608 Galicia (NW Spain). *Diseases of Aquatic Organisms* **46**, 47-55.
- 609 **Iglesias, R., Paramá, A., Álvarez, M.F., Leiro, J., Aja, C. and Sanmartín, M.L.**
 610 (2003). *In vitro* growth requirements for the fish
 611 pathogen *Philasterides dicentrarchi* (Ciliophora, Scuticociliatida). *Veterinary*
 612 *Parasitology* **111**:19-30.
- 613 **Ito, H., Fukuda, Y., Murata, K. and Kimura, A.** (1983). Transformation of intact
 614 yeast cells treated with alkali cations *Journal of Bacteriology* **153**, 163–168

- 615 **Karlsson, J.** (1975). Membrane-bound potassium and magnesium ion-stimulated
616 inorganic pyrophosphatase from roots and cotyledons of sugar beet (*Beta*
617 *vulgaris* L.). *Biochimica et Biophysica Acta* **399**, 356-363.
- 618 **Kim, Y., Kim, E.J. and Rea, P.A.** (1994). Isolation and characterization of cDNAs
619 encoding the vacuolar H⁺-pyrophosphatase of *Beta vulgaris*. *Plant Physiology*
620 **106**, 375-382.
- 621 **Kimura, M.** (1980). A simple method for estimating evolutionary rates of base
622 substitutions through comparative studies of nucleotide sequences. *Journal of*
623 *Molecular Evolution* **16**, 111-120.
- 624 **Lerchl, J., König, S., Zrenner, R. and Sonnewald, U.** (1995). Molecular cloning,
625 characterization and expression of isoforms encoding tonoplast-bound proton-
626 translocating inorganic pyrophosphatase in tobacco. *Plant Molecular Biology* **28**,
627 833-840.
- 628 **Livak, K.J. and Schmittgen, T.D.** (2001). Analysis of relative gene expression data
629 using real-time quantitative PCR and the 2^{-ΔΔC_T} Method. *Methods* **25**, 402-408.
- 630 **Long, A.R., Williams, L.E., Nelson, S.J. and Hall, J.L.** (1995). Localization of
631 membrane pyrophosphatase activity in *Ricinus communis* seedlings. *Journal of*
632 *Plant Physiology* **146**, 629-638.
- 633 **López-López, O., Fuciños, P., Pastrana, L., Rúa, M.L., Cerdán, M.E. and**
634 **González-Siso, M.I.** (2010). Heterologous expression of an esterase from
635 *Thermus thermophilus* HB27 in *Saccharomyces cerevisiae*. *Journal of*
636 *Biotechnology* **145**, 226-232.
- 637 **Luo, S., Marchesini, N., Moreno, S.N. and Docampo, R.** (1999). A plant-like vacuolar
638 H(+)-pyrophosphatase in *Plasmodium falciparum*. *FEBS Letters* **460**, 217-220.

- 639 **Maeshima, M.** (2000). Vacuolar H⁺-pyrophosphatase. *Biochimica et Biophysica Acta*
640 **1465**, 37-51.
- 641 **Mallo, N., Lamas, J. and Leiro, J.M.** (2013). Evidence of an alternative oxidase
642 pathway for mitochondrial respiration in the scuticociliate *Philasterides*
643 *dicentrarchi*. *Protist* **164**, 824-836.
- 644 **Mallo, N., Lamas, J., Piazzon, C. and Leiro, J.M.** (2015). Presence of a plant-like
645 proton-translocating pyrophosphatase in a scuticociliate parasite and its role as a
646 possible drug target. *Parasitology* **142**, 449-462.
- 647 **Marchesini, N., Luo, S., Rodrigues, C.O., Moreno, S.N.J. and Docampo, R.** (2000).
648 Acidocalcisomes and vacuolar H⁺-pyrophosphatase in malaria parasites.
649 *Biochemical Journal* **347**, 243-253.
- 650 **MacIntosh, M.T., Drozdowicz, Y.M., Laroiya, K., Rea, P.A. and Vaidya, A.B.**
651 (2001). Two classes of plant-like vacuolar-type H(+)-pyrophosphatases in
652 malaria parasites. *Molecular and Biochemical Parasitology* **114**, 183-195.
- 653 **Mitsuda, N., Enami, K., Nakata, M., Takeyasu, K. and Sato, M.H.** (2001). Novel
654 type *Arabidopsis thaliana* H⁺-PPase is localized to the Golgi apparatus. *FEBS*
655 *Letters* **488**, 29-33.
- 656 **Moreno, S.N.J. and Docampo, R.** (2009). The role of acidocalcisomes in parasitic
657 protists. *Journal of Eukaryotic Microbiology* **56**, 208-213.
- 658 **Moriyama, Y., Hayashi, M., Yatsushiro, S. and Yamamoto, A.** (2003).
659 Vacuolar proton pumps in malaria parasite cells. *Journal of Bioenergetics and*
660 *Biomembranes* **35**: 367-375.
- 661 **Motamayor, J.C., Mockaitis, K., Schmutz, J., Haiminen, N., Livingstone,**
662 **D., Cornejo, O., Findley, S.D., Zheng, P., Utró, F., Royaert, S., Saski,**
663 **C., Jenkins, J., Podicheti, R., Zhao, M., Scheffler, B.E., Stack, J.C., Feltus,**

- 664 F.A., Mustiga, G.M., Amores, F., Phillips, W., Marelli, J.P., May,
665 G.D., Shapiro, H., Ma, J., Bustamante, C.D., Schnell, R.J., Main,
666 D., Gilbert, D., Parida, L. and Kuhn, D.N. (2013) The genome sequence of the
667 most widely cultivated cacao type and its use to identify candidate genes
668 regulating pod color. *Genome Biology* **14**, r53.
- 669 Pérez-Castiñeira, J.R., Gómez-García, R., López-Marqués, R.L., Losada, M. and
670 Serrano, A. (2001) Enzymatic systems of inorganic pyrophosphatase
671 bioenergetics in photosynthetic and heterotrophic protists: remnants or metabolic
672 cornerstones? *International Microbiology* **4**, 135-142.
- 673 Pérez-Castiñeira, J.R., Alvar, J., Ruiz-Pérez, L.M. and Serrano, A. (2002).
674 Evidence for a wide occurrence of proton-translocating pyrophosphatase genes
675 in parasitic and free-living protozoa. *Biochemical and Biophysical Research*
676 *Communications* **294**, 567-573.
- 677 Philimonenko, V.V., Janáček, J. and Hozák, P. (2002). LR White is preferable to
678 Unicryl for immunogold detection of fixation sensitive nuclear antigens.
679 *European Journal of Histochemistry* **46**, 359-364.
- 680 Piazzón, C., Lamas, J., Castro, R., Budiño, B., Cabaleiro, S., Sanmartín, M.L.
681 and Leiro, J. (2008). Antigenic and cross-protection studies on two turbot
682 scuticociliate isolates. *Fish and Shellfish Immunology* **25**, 417-424.
- 683 Piazzon, C., Lamas, J. and Leiro, J.M. (2011). Role of scuticociliate proteinases in
684 infection success in turbot, *Psetta maxima* (L.). *Parasite Immunology* **33**, 535-
685 544.
- 686 Plattner, H., Sehring, I.M., Mohamed, I.K., Miranda, K., De Souza, W., Billington,
687 R., Genazzani, A. and Ladenburger, E.M. (2012) Calcium signaling in closely
688 related protozoan groups (Alveolata): non-parasitic ciliates (*Paramecium*,

- 689 *Tetrahymena*) vs. parasitic Apicomplexa (*Plasmodium*, *Toxoplasma*). *Cell*
690 *Calcium* **51**, 351-382.
- 691 **Poulos, M.G., Batra, R., Charizanis, K. and Swanson, M.S.** (2011). Developments in
692 RNA splicing and disease. *Cold Spring Harbor Perspectives in Biology* **3**,
693 a000778.
- 694 **Rea, P.A. and Poole, R.J.** (1993). Vacuolar H⁺-translocating pyrophosphatase. *Annual*
695 *Review of Plant Physiology and Plant Molecular Biology* **44**, 157-180.
- 696 **Rea, P.A., Kim, Y., Sarafian, V., Poole, R.J., Davies, J.M. and Sanders, D.** (1992).
697 Vacuolar H⁺-translocating pyrophosphatases: a new category of ion translocase.
698 *Trends in Biochemical Sciences* **17**, 348-353.
- 699 **Robinson, D.G., Haschke, H.P., Hinz, G., Hoh, B., Maeshima, M. and Marty, F.**
700 (1996). Immunological detection of tonoplast polypeptides in the plasma
701 membrane of pea cotyledons. *Planta* **198**, 95-103.
- 702 **Saitoh, O., Murata, Y., Odagiri, M., Itoh, M., Itoh, H., Misaka, T. and Kubo, Y.**
703 (2002). Alternative splicing of RGS8 gene determines inhibitory function of
704 receptor type-specific Gq signaling. *Proceedings of the National Academy of*
705 *Sciences USA* **99**, 10138-10143.
- 706 **Saliba, K.J., Allen, R.J., Zissis, S., Bray, P.G., Ward, S.A. and Kirk, K.** (2003).
707 Acidification of the malaria parasite's digestive vacuole by a H⁺-ATPase and a
708 H⁺-pyrophosphatase. *The Journal of Biological Chemistry* **278**, 5605-5612.
- 709 **Sarafian, V., Kim, Y., Poole, R.J. and Rea, P.A.** (1992). Molecular cloning and
710 sequence of cDNA encoding the pyrophosphate-energized vacuolar membrane
711 proton pump of *Arabidopsis thaliana*. *Proceedings of the National Academy of*
712 *Sciences USA* **89**, 1775-1779.

- 713 **Scott, D.A. and Docampo, R.** (2000). Characterization of isolated acidocalcisomes of
714 *Trypanosoma cruzi*. *The Journal of Biological Chemistry* **275**, 24215-24221.
- 715 **Serrano, A., Pérez-Castiñeira, R., and Baltscheffsky, H.** (2004). Proton-pumping
716 inorganic pyrophosphatases in some archaea and other extremophilic prokaryotes.
717 *Journal of Bioenergetics and Biomembranes* **36**, 127-133.
- 718 **Serrano, A, Pérez-Castiñeira, J.R., Baltscheffsky, M. And Baltscheffsky, H.** (2007).
719 H^+ -PPases: yesterday, today and tomorrow. *IUBMB Life* **59**, 76-83.
- 720 **Sievers, F., Wilm, A., Dineen, D., Gibson, T.J., Karplus, K., Li, W., López, R.,**
721 **McWilliam, H., Remmert, M., Söding, J., Thompson, J.D. and Higgins, D.G.**
722 (2011). Fast, scalable generation of high-quality protein multiple sequence
723 alignments using Clustal Omega. *Molecular Systems Biology* **7**, 539.
- 724 **Silva, P. and Gerós, H.** (2009). Regulation by salt of vacuolar H^+ -ATPase and H^+ -
725 pyrophosphatase activities and Na^+/H^+ Exchange. *Plant Signaling and Behavior*
726 **4**, 718-726.
- 727 **Scott, D.A., de Souza, W., Benchimol, M., Zhong, L., Lu, H.G., Moreno, S.N. and**
728 **Docampo, R.** (1998). Presence of a plant-like proton-pumping pyrophosphatase
729 in acidocalcisomes of *Trypanosoma cruzi*. *The Journal of Biological Chemistry*
730 **273**, 22151-22158.
- 731 **Sakakibara, Y., Kobayashi, H. and Kasamo, K.** (1996). Isolation and characterization
732 of cDNAs encoding vacuolar H^+ -pyrophosphatase isoforms from rice (*Oryza*
733 *sativa* L.). *Plant Molecular Biology* **31**, 1029-1038.
- 734 **Tamura, K., Stecher, G., Peterson, D., Filipski, A. and Kumar, S.** (2013). MEGA6:
735 Molecular Evolutionary Genetics Analysis version 6.0. *Molecular Biology and*
736 *Evolution* **30**, 2725-2729.

737 **Venter, M., Gronewald, J.-H. and Botha, F.C.** (2006). Sequence analysis and
738 transcriptional profiling of two vacuolar H⁺-pyrophosphatase isoforms in *Vitis*
739 *vinífera*. *Journal of Plant Research* **119**, 469-478.

740

741

For Peer Review

742 FIGURE LEGENDS

743

744 **Figure 1.** A, B) Immunofluorescence detection by confocal microscopy of H^+ -PPase in
 745 a ciliate trophozoite using a mouse antibody anti- recombinant H^+ -PPase expressed in
 746 yeast *Saccharomyces cerevisiae* and a secondary polyclonal antibody anti-mouse Ig
 747 conjugated with FITC. After immunofluorescence assay, trophozoites were
 748 counterstained with DAPI to identify the macronucleus (M). A) Arrows indicate the
 749 immunolocalization of H^+ -PPase in the vacuoles and arrowhead indicate the presence of
 750 a specific immunostaining appears as a dotted line coinciding with the alveolar sacs. B)
 751 Fluorescent staining of acidic compartiments of *P. dicentrarchi* using Lysotracker Red
 752 DND-99 show a fluorescent staining of the posterior vacuoles (arrows) and the alveolar
 753 sacs (arrowhead). Scale bars = 10 μ m.

754

755 **Figure 2.** Immunofluorescence detection by confocal microscopy of H^+ -PPase isoform
 756 (H^+ -PPase2) with PAB_{HK} polyclonal antibody (A) and anti-AVP1 polyclonal antisera
 757 (B) where you can see a pattern of discontinuous fluorescence on the surface of
 758 trophozoites (arrowhead). C,D) Immunoelectromicroscopy localization of the isoform
 759 H^+ -PPase2 using the polyclonal PAB_{HK} antibody corresponding to AVP1 isoform of *A.*
 760 *thaliana* and which shows a specific staining (arrowhead) on the membrane of the
 761 alveolar sacs.

762

763 **Figure 3.** A) Nucleotide sequence belonging to a gene region of the H^+ -PPase of *P.*
 764 *dicentrarchi* together with its corresponding translation into amino acids, containing a
 765 sequence motif recognized by the antibody PAB_{HK} (box in black). In the lower part of
 766 the figure are shown the products of PCR and RT-PCR obtained usign ADN and RNA

as template and the primers FPiPh/RPiPh, analyzed on agarose gel 4% being observed in the case of using cDNA as template, the presence of two bands that correspond, respectively to isoform 1 (the larger), and 2 (the smallest) and containing this last the complete motif recognized by the polyclonal antibody PAB_{HK}. B) Western blot with antibody PAB_{HK} (lane 1) on ciliate membrane-associated proteins (MAPs) of trophozoites subjected to SDS-PAGE under nonreducing conditions and which recognizes a single band of approximately 62 kD (arrow). Mw: Molecular weight markers.

Figure 4. A) Multiple sequence alignment using Clustal Omega program of aa sequences obtained from a partial ORF of the gene of H⁺-PPasa from several isolates (B₁, D₂, D₃, C₁, I₁, S₁ y P₁) of *P. dicentrarchi*. The boxes in bold indicate the motif recognized by the antibody PAB_{HK}. B) Phylogenetic comparison of H⁺-PPase of *P. dicentrarchi* isolates. Aligned Aa sequences were subjected to phylogenic analysis with neighbor joining (NJ) method. The numbers at the nodes represent bootstrap values out of 1000 resampled values in the NJ analysis with the Kimura two-parameter correction model.

Figure 5. Relative gene expression levels of H⁺-PPase of *P. dicentrarchi* determined by RT-qPCR in trophozoites incubated for 24 h in medium containing different concentrations of NaCl: 4, 8 and 37 ‰. Gene expression was normalized to reference gene α -tubulin of *P. dicentrarchi* and normalized data are expressed in arbitrary units. Values shown are means \pm standard error (E.S.) of five assays. **P* < 0.01 relative to ciliates incubated in the medium containing a salt concentration of 37 ‰.

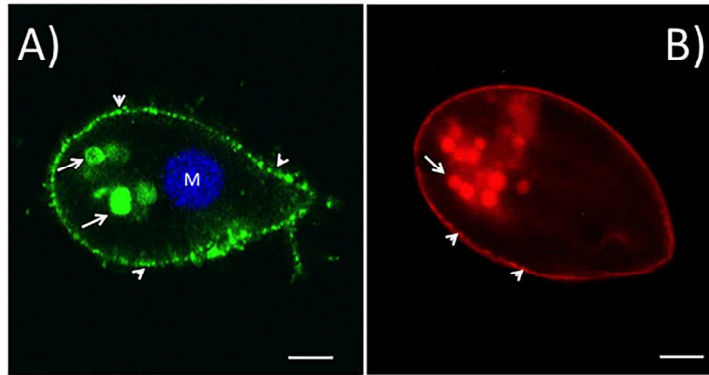


Figure 1

119x90mm (300 x 300 DPI)

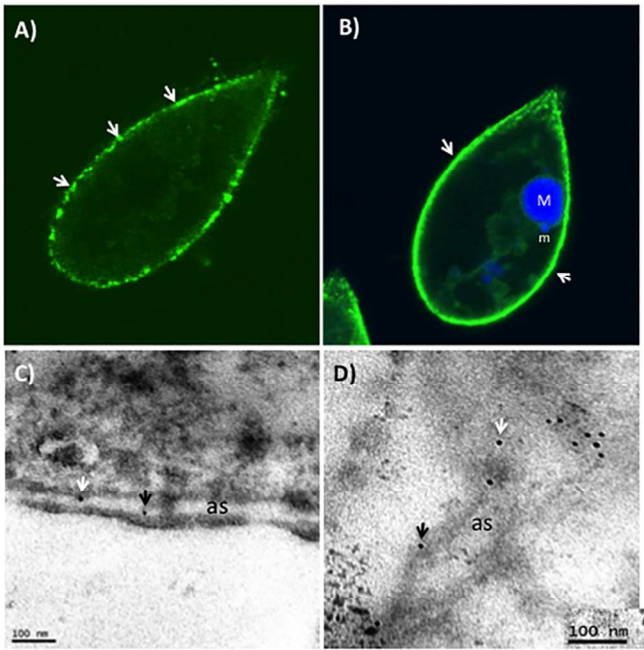
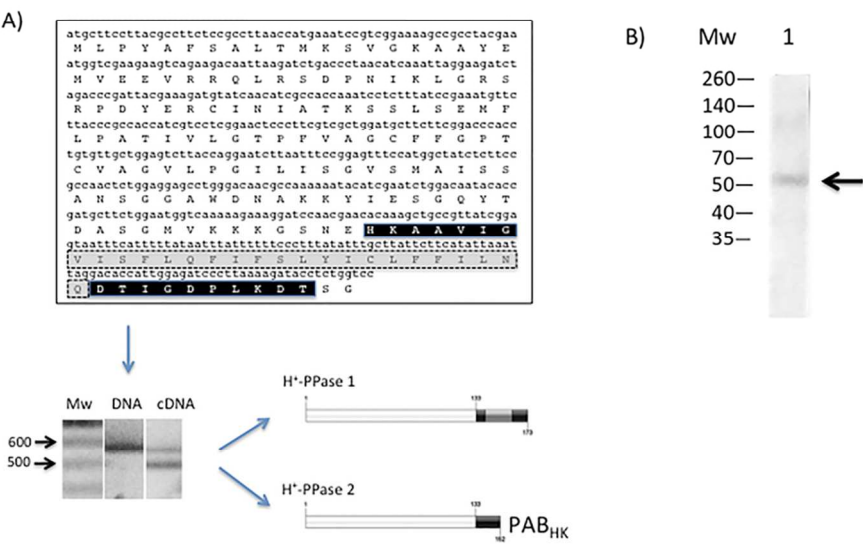


Figure 2

119x90mm (300 x 300 DPI)



A)

D2	MLPYAFSALTMKSVGKAAAYEMVEEVRRLRSDPNIKLGRSRPDYERCINIATKSSLSEMF
I1	MLPYAFSALTMKSVGKAAAYEMVEEVRRLRSDPNIKLGRSRPDYERCINIATKSSLSEMF
B1	MLPYAFSALTMKSVGKAAAYEMVEEVRRLRSDPNIKLGRSRPDYERCINIATKSSLSEMF
D3	MLPYAFSALTMKSVGKAAAYEMVEEVRRLRSDPNIKLGRSRPDYERCINIATKSSLSEMF
P1	MLPYAFSALTMKSVGKAAAYEMVEEVRRLRSDPNIKLGRSRPDYERCINIATKSSLSEMF
S1	MLPYAFSALTMKSVGKAAAYEMVEEVRRLRSDPNIKLGRSRPDYERCINIATKSSLSEMF
C1	MLPYAFSALTMKSVGKAAAYEMVEEVRRLRSDPNIKLGRSRPDYERCINIATKSSLSEMF

D2	LPATIVLGTFFVAGCFFGPTCVAGVLPGLISGVSMIAISSANGGAWDNAKKYIESGQYT
I1	LPATIVLGTFFVAGCFFGPTCVAGVLPGLISGVSMIAISSANGGAWDNAKKYIESGQYT
B1	LPATIVLGTFFVAGCFFGPTCVAGVLPGLISGVSMIAISSANGGAWDNAKKYIESGQYT
D3	LPATIVLGTFFVAGCFFGPTCVAGVLPGLISGVSMIAISSANGGAWDNAKKYIESGQYT
P1	LPATIVLGTFFVAGCFFGPTCVAGVLPGLISGVSMIAISSANGGAWDNAKKYIESGQYT
S1	LPATIVLGTFFVAGCFFGPTCVAGVLPGLISGVSMIAISSANGGAWDNAKKYIESGQYT
C1	LPATIVLGTFFVAGCFFGPTCVAGVLPGLISGVSMIAISSANGGAWDNAKKYIESGQYT

D2	DASGMVKKKGSNEBKAAVIIVISFLQFIFSLYICLFFILNDTIGDPLKDTSG
I1	DASGMVKKKGSNEBKAAVIIVISFLQFIFSLYICLFFILNDTIGDPLKDTSG
B1	DASGMVKKKGSNEBKAAVIIVISFLQFIFSLYICLFFILNDTIGDPLKDTSG
D3	DASGMVKKKGSNEBKAAVIIVISFLQFIFSLYICLFFILNDTIGDPLKDTSG
P1	DASGMVKKKGSNEBKAAVIIVISFLQFIFSLYICLFFILNDTIGDPLKDTSG
S1	DASGMVKKKGSNEBKAAVIIVISFLQFIFSLYICLFFILNDTIGDPLKDTSG
C1	DASGMVKKKGSNEBKAAVIIVISFLQFIFSLYICLFFILNDTIGDPLKDTSG

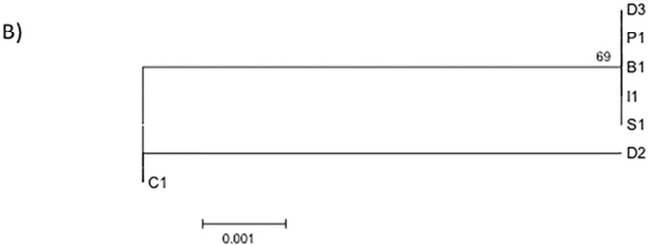


Figure 4

90x67mm (300 x 300 DPI)

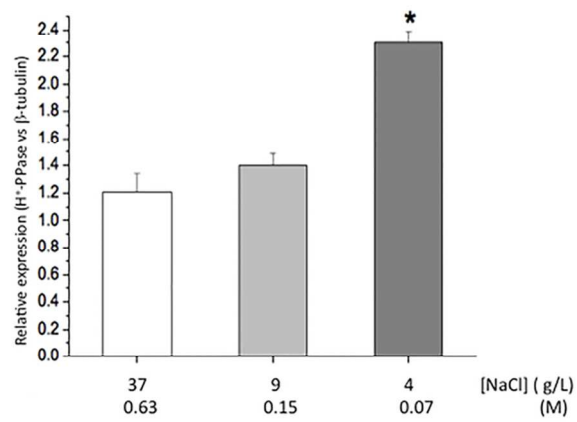


Figure 5

90x67mm (300 x 300 DPI)